Stem Cells Translational Medicine, 2023, **12**, 154–168
https://doi.org/10.1093/stcltm/szad007
Advance access publication 8 March 2023
Original Research

Exosome-Based Regimen Rescues Endometrial Fibrosis in Intrauterine Adhesions Via Targeting Clinical Fibrosis Biomarkers

Yifeng Lin[1,‡], Yaoshen Li[2,‡], Panpan Chen[1,‡], Yanye Zhang[3], Jiwei Sun[3], Xiao Sun[3], Jiaqun Li[3], Jiani Jin[3], Jinglei Xue[3], Junyan Zheng[3], Xin-Chi Jiang[2,4], Chuan Chen[3], Xiaoqing Li[3], Yiqing Wu[3], Wei Zhao[3], Juan Liu[3], Xiaohang Ye[3], Runju Zhang[*,1,3], Jianqing Gao[*,2,4,5], Dan Zhang[*,1,3]

[1]Key Laboratory of Reproductive Genetics (Ministry of Education) and Department of Reproductive Endocrinology, Women's Hospital, Zhejiang University School of Medicine, Hangzhou, Zhejiang, People's Republic of China
[2]Institute of Pharmaceutics, College of Pharmaceutical Sciences, Zhejiang University, Hangzhou, People's Republic of China
[3]Key Laboratory of Women's Reproductive Health of Zhejiang Province and Department of Reproductive Endocrinology, Women's Hospital, Zhejiang University School of Medicine, Hangzhou, Zhejiang, People's Republic of China
[4]Dr Li Dak Sum & Yip Yio Chin Center for Stem Cell and Regenerative Medicine, Zhejiang University, Hangzhou, People's Republic of China
[5]Jinhua Institute of Zhejiang University, Jinhua, People's Republic of China

[*]Corresponding author: Dan Zhang, PhD, Key Laboratory of Reproductive Genetics (Ministry of Education) and Department of Reproductive Endocrinology, Women's Hospital, Zhejiang University School of Medicine, Hangzhou, Zhejiang Province 310006, People's Republic of China. Email: zhangdan@zju.edu.cn; or, Jianqing Gao, PhD, Institute of Pharmaceutics, College of Pharmaceutical Sciences, Zhejiang University, Hangzhou, Zhejiang Province 310058, People's Republic of China. Email: gaojianqing@zju.edu.cn; or, Runju Zhang, PhD, Key Laboratory of Reproductive Genetics (Ministry of Education) and Department of Reproductive Endocrinology, Women's Hospital, Zhejiang University School of Medicine, Hangzhou, Zhejiang Province, 310006, People's Republic of China. Email: 5311005@zju.edu.cn
[‡]Contributed equally as co-first authors.

Abstract

Intrauterine adhesions (IUA), which is characterized by endometrial fibrosis, continue to be the most common cause of uterine infertility globally. Our work revealed that 3 fibrotic progression markers (Vimentin, COL5A2, and COL1A1) were significantly increased in the endometrium of IUA patients. Mesenchymal stem cell–derived exosomes (EXOs) have been recently revealed as a cell-free therapy for fibrosis diseases. Nevertheless, the application of EXOs is restricted by the short residency duration in the target tissue. To overcome this limitation, herein, we reported an exosome–based regimen (EXOs-HP) that thermosensitive poloxamer hydrogel possessed the ability to efficiently promote the residency duration of EXOs in the uterine cavity. By downregulating fibrotic progression markers (Vimentin, COL5A2, and COL1A1), EXOs-HP could significantly restore the function and structure of the injured endometrium in the IUA model. Our work provides the theoretical and experimental foundation of EXOs-HP in treating IUA, highlighting the clinical potential of topical EXOs-HP delivery system in IUA patients.

Key words: intrauterine adhesions; endometrial fibrosis; fibrosis biomarkers; exosomes; poloxamer hydrogel.

Received: 21 August 2022; Accepted: 17 January 2023.

Graphical Abstract

In this study, we identified 3 upregulated fibrotic progression markers (Vimentin, COL5A2, and COL1A1) in the endometrium of IUA patients and highlighted the efficacious therapy of EXOs–HP via inhibiting the fibrosis process.

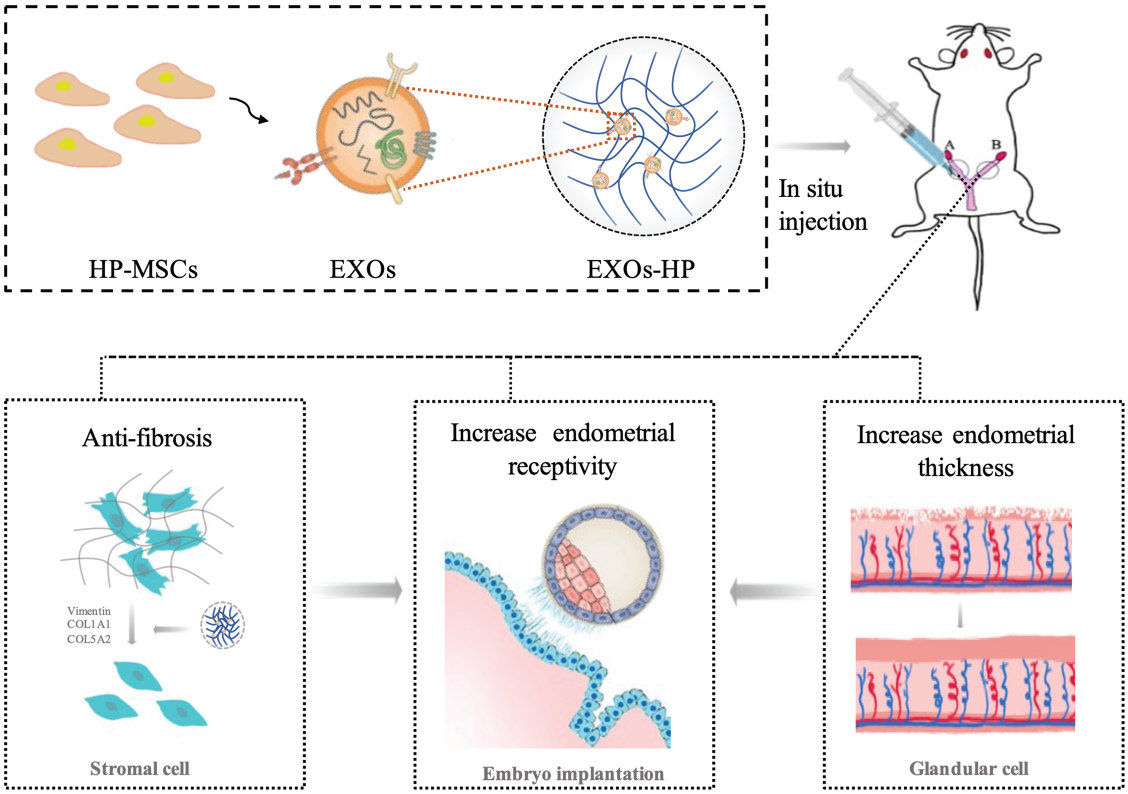

Significance Statement

The challenge of anti-intrauterine adhesion (IUA) treatment development is rescuing the fibrosis progress of endometrium. Therefore, we investigated the expression of clinical fibrotic progression markers (Vimentin, COL5A2, and COL1A1) in the endometrium of IUA patients, which can serve as promising pathological predictors and therapeutic targets for patients with IUA. Furthermore, we revealed that EXOs-HP (mesenchymal stem cell-derived exosomes encapsulated in heparin-poloxamer hydrogel) delivery system could rescue IUA via attenuating the fibrotic markers.

Introduction

Intrauterine adhesion (IUA), a common type of gynecological disease, is the leading cause of uterine-related infertility with the increase of intrauterine surgeries and poses severe negative impacts on reproductive-aged women's physical and mental health.[1-4] The most common causes of IUA are endometrium damage-induced fibrosis, which usually occurs after dilatation and curettage after postpartum hemorrhage, pregnancy loss, or induced abortion.[5]

The pathological characteristics of IUA are endometrial fibrosis and excessive extracellular matrix (ECM) deposition.[6-8] A range of treatments have been explored to reduce endometrial fibrosis, including transcervical resection of adhesions, intrauterine contraceptive devices, anti-adhesive barriers, and periodic hormone treatments. But the clinical efficacy of these approaches is unsatisfactory, the recurrence rate of IUA is still high (3.1%-23.5%), especially in cases with a severe degree of adhesions, with recurrence rates as high as 20%-62.5%.[9,10] Therefore, it is urgent to develop efficacious treatments to reduce endometrial fibrosis and improve endometrial receptivity.

Exosomes are extracellular vesicles with a diameter of 30-150 nm that transports bioactive proteins, mRNA, and microRNA across cells to induce biological reactions in recipient cells. Stem cell derived-exosomes therapy represents an emerging alternative source for the treatment of numerous diseases, including endometrial fibrosis.[11-13] Our previous research has demonstrated that human placenta-derived mesenchymal stem cells (HP-MSCs) promoted endometrial regeneration via promoting epithelial and stromal cell proliferation in an endometrium-injured mouse.[14] However, the mechanisms of HP-MSC interacting with endometrial cells remain unknown. Exosomes contain a large number of components from their original cells and serve as an important paracrine factor for cell-to-cell communication. TGF-β1 is a key signaling regulator in the pathogenesis of fibrosis. Several studies have reported that TGF-β1 is activated in the endometrial tissue of IUA patients or animal models.[15-17] TGF-β1 stimulates an increase in expression levels involved in fibrogenesis, including Smad2/3, α-SMA, fibronectin, vimentin, COL1A1, etc.[12,18,19] Based on these, we hypothesized that HP-MSCs-derived exosomes may be involved in reducing

endometrial fibrosis by antagonizing TGF-β1 induced fibrosis in IUA.

However, therapeutics based on exosomes have short life and retention time in tissue. To overcome these limitations, we adopted thermosensitive poloxamer hydrogel (HP) to enhance the retention time of delivered exosomes. HP is a form of biocompatible and bioactive material that is approved by the US Food and Drug Administration (FDA) to use in clinical applications. In our work, we used poloxamer 407 and poloxamer 188 for the manufacture of thermosensitive hydrogel to promote the retention and stability of HP-MSCs–derived exosomes (EXOs) in the endometrium.

Hence, the present study aimed to identify the fibrosis markers in IUA patients' endometrium and explore whether EXOs loaded with HP (EXOs-HP) can restore the fibrotic endometrium. Specifically, we investigated the following: (1) identify the expression of fibrotic markers in IUA patients, (2) determine the therapeutic effect of EXOs-HP on the IUA mouse model, (3) explore the effect of EXOs on rescuing TGF-β1 induced IUA cell model, and (4) explore the effect of EXOs on the proliferation of human endometrial glandular cells. Our data revealed that EXOs-HP represents a novel approach with great clinical potential by promoting endometrial regeneration after injury.

Materials and Methods

The research protocol was approved by the Ethics Committee of Women's Hospital School of Medicine Zhejiang University, China and the Laboratory Animal Center of Zhejiang University, China. Written informed consent was obtained from all participants before tissue collection. All animal research, feeding, processing, stem cell instillation, sample collection, and experimental procedures were carried out following the principles and procedures of the Women's Hospital of Zhejiang University, China. We confirmed that the human and animal studies in our experiments were carried out under the relevant guidelines and regulations approved by the Women's Hospital of Zhejiang University (IRB-20210047-SC) and Laboratory Animal Center of Zhejiang University (ZJU20210175), China.

Patient Samples of Endometrium

Between January 2017 and January 2022, 38 female patients aged 25-45 years with moderate-to-severe IUA at Zhejiang University's Women's Hospital were enrolled in our study. The criteria for patient inclusion were hysteroscopic adhesion scores for moderate-to-severe IUA (the score ranged from 5 to 12) according to the American Reproductive Association's objective scoring standard. A total of 37 female patients aged 25-45 years with normal endometrium and no adhesion who had received a hysteroscopic examination for a routine infertility test were selected as controls. Patients were excluded from the study if they had any of the following conditions: hysteroscopy contraindications, chromosome karyotype abnormalities, congenital uterine malformations, severe adenomyosis, pregnancy contraindications, a medical history of malignant pelvic tumors, or previous experience with pelvic radiotherapy. The endometrium taken from the whole body of the uterus was collected during the proliferating phase of the menstrual cycle by endometrial biopsy.

Isolation and Identification of HP-MSCs

Identified MSCs were kindly provided by the College of Life Sciences-iCell Biotechnology Regenerative Biomedicine Laboratory, Zhejiang University. The identification results of these HP-MSCs were provided in Supplementary Fig. S3.

Exosome Isolation and Characterization

For exosome preparation, HP-MSCs were cultured in basic DMEM/F12 medium (Hyclone, Logan, USA) containing 10% fetal bovine serum (FBS, Biological Industries, Kibbutz Beit-Haemek, Israel), 1% penicillin (Geno, Hangzhou, China) at 5% CO_2, and 37 °C as previously optimized.[20,21] After growing to 60%-70%, the HP-MSCs were washed with serum-free DMEM/F12 and cultured with serum-free DMEM/F12 for 48 h. To isolate the exosomes, conditioned medium (CM) was collected and undergoes differential centrifugation at 4 °C as follows: 300 *g* for 5 min, 2000 *g* for 30 min, 10 000 *g* for 30 min, 100 000 *g* for 70 min, and then pellet was washed with PBS and centrifuged at 100 000 *g* for 70 min twice.[22-24] Exosomes were re-suspended in PBS and then preserved at −80 °C. The particle size of the final exosomes was measured by nanoparticle tracking analysis measurements using Mastersizer 2000 (Malvern, USA). The morphology of the exosomes was verified by transmission electron microscopy (TEM, G2 Spirite 120 kV, FEI Technai, USA). A drop of exosome pellet (20 μL) was absorbed by a carbon film, followed by incubation for 5 min at room temperature, and 2% phosphotungstic acid was used for negative staining. Samples were then air-dried for image capturing by TEM. To quantify the final concentration of exosomes, a BCA Protein Assay Kit (Applygen) was used to measure. Exosome-associated markers were detected by Western blot assay, and the primary antibodies included CD63 (ET1607-2, HuaBio, China) and CD9 (ET1601-9, HuaBio, China).

Exosome-Loaded HP Construction and Rheological Measurements

Poloxamer 407 powder (Sigma, USA) was dissolved in the appropriate volume of PBS to the target concentration of 17.5% (w/w) and then stirred in an ice bath. After poloxamer 407 powder was completely dissolved, 2% (w/w) poloxamer 188 was added to the solution. The mixture was then stored at 4 °C until poloxamer 188 was dissolved to get HP. EXOs were then added to HP at the ratio of 100 μg exosome per 1 mL HP. The mixture was then blended with a shaker at 100 g for 10 min to get EXOs-HP. Rheological properties of HP and EXOs-HP were measured with a rheometer (MCR302e, Aton paar, Austria) at different temperatures from 30 °C to 42 °C or at 37 °C for different time points. The elastic modulus and viscous shear modulus of HP and EXOs-HP were determined with a stainless steel parallel flat plate (25 mm) at 1 rad s^{-1}.

In Vitro Release of EXOs-HP

HP loaded with the 2 μg mL^{-1} commercial red fluorescent probe CM-DiD (US Everbright, Inc., Jiangsu, China) labeled exosomes were incubated at 37 °C. After gelling, 10 times the volume of 37 °C PBS was added. The supernatant was collected at different time points (0, 0.5, 1, 2, 4, 8, 12, 24, 48, and 72 h), and the same volume of fresh PBS was replenished. The content of exosomes in the supernatant was determined by fluorescence quantification. After the last time points,

the remained supernatant was collected and centrifuged at 10 000*g* for 1 h. A TEM (G2 Spirite 120 kV, FEI Technai, USA) was used to observe the morphology of exosomes in precipitation after being released from HP. Western blot analysis was used to detect the exosome-associated markers changes (CD9 and CD63) after EXOs were released from HP.

Isolation and Identification of Human Stromal and Glandular Cells

Twenty female patients aged between 24 and 48 years old with normal menstrual cycles (21-35 days) were recruited at the Women's Hospital of Zhejiang University, China. They did not receive hormone therapy for at least 3 months before surgery. All the patients underwent hysteroscopy and endometrial biopsy during the infertility examination. Primary human endometrial stromal cells (HESCs) and glandular cells were isolated from the endometrium as previously described.[25] Both groups of cells were cultured in DMEM/F12 medium containing 10% FBS and 1% Penicillin-Streptomycin at 37 °C in a humidified environment with 5% CO_2. The medium was replaced every 2-3 days, and the cells were passaged at a 1:3-1:4 ratio and cryopreserved.[26] The human primary endometrial gland cells and stromal cells were identified by immunofluorescence (IF) of CK7 (Abcam, ab68459) and Vimentin (CST, 5741), as shown in Supplementary Fig. S4.

EdU Proliferation Assay

Human glandular cells were plated in 24-well plates and added 150 μg mL^{-1} exosomes. After 24, 48, and 72 h, the cell proliferation activity was assessed using a commercially available EdU Assay Kit (RIBOBIO, Guangdong, China) according to the protocol provided. Cell proliferation was quantified by incorporating EdU into the newly synthesized DNA of replicating cells. The proliferated cells were dyed red, while the nuclei of all cells were dyed blue with DAPI. By counting EdU/DAPI ratio, cell proliferation ability can be assessed.

Immunofluorescence

Treated HESCs were fixed in 4% paraformaldehyde for 4 min, washed with PBS 3 times, incubated with 0.5% Triton-100 at room temperature for 20 minutes, and washed 3 times. The cells were blocked in bovine serum albumin (BSA; 5%) for 20 minutes at room temperature, and the blocking solution was then removed. Antibodies against COL1A1 (39952, Cell Signaling Technology, Boston, USA), Vimentin (5741, Cell Signaling Technology, Boston, USA), and COL5A2 (ER65613, HuaBio, Hangzhou, China) were added. The cells were incubated overnight in a humidified incubator at 4 °C. The next day, the primary antibody was discarded, the cells were washed 3 times with PBS, and a goat anti-rabbit secondary antibody was added. The cells were incubated with the secondary antibody at 37 °C for 30 minutes, followed by 3 washes with PBS. DAPI staining was performed in the dark at room temperature. The sections were observed and photographed under Olympus IX81-FV100 (Olympus, Japan).

Development of an IUA Cell Model (TGF-β1-Treated HESCs)

Cytokine TGF-β1 (100-21) was brought from PEPROTECH (Waltham, MA, USA). TGF-β1 was applied to HESCs for 12, 24, 48, and 72 h at different concentrations (0, 2.5, 5, 10, 20, and 40 ng mL^{-1}). The protein expression level of Vimentin, COL5A2, and COL1A1 was detected by WB and IF. The mRNA expression levels of Vimentin, COL5A2, COL1A1, α-SMA, MMP2, and TGF-βR were detected by RT-qPCR.

RT-qPCR

Total RNA was extracted from HESCs using Trizol according to the manufacturer's protocol (Invitrogen, USA). About 1 μg RNA was converted to cDNA by the MMLV Reverse Transcriptase cDNA Synthesis Kit (Vazyme, Nanjing, China). Real-time qPCR was carried out using the Roche LightCycler 480II. Primers used for RT-qPCR assay are shown in Supplementary Table S1. Results were normalized to Gapdh expression and analyzed using the comparative threshold cycle method.

Protein Isolation and Western Blot Analysis

Both the human endometrium and treated HESCs were lysed using RIPA lysis buffer (Cell Signaling Technology, Boston, USA) as described previously.[25] A bicinchoninic acid protein assay kit was used to determine the protein content (Thermo Scientific, Waltham, MA, USA). Proteins were denatured in a 5× SDS-PAGE loading buffer (CWBIO, Beijing, China). Then they were separated on sodium dodecyl sulfate-polyacrylamide gels and subsequently transferred onto nitrocellulose membranes. After blocking with 5% BSA in PBS, the membranes were incubated with primary and secondary antibodies. Next, the immunoblots were washed with PBST (PBS with 0.1% Tween-20). And then, the membranes were incubated overnight with primary antibodies at 4 °C. After washing, secondary antibodies were added and incubated at room temperature for 1 h in the dark. Finally, the membranes were probed with an Odyssey CLx (LI-COR, USA) and ChemiDoc Touch Imaging System (Bio-Rad, USA). The signal intensity was calculated with ImageStudio. Protein expression was normalized to β-actin. Antibodies against COL1A1 (39952) and Vimentin (5741) were added were purchased from Cell Signaling Technology. Antibody COL5A2 (ER65613) was purchased from HuaBio.

Establishment of the IUA Mouse Model

Female ICR mice aged 8 weeks (SLAC company, Shanghai) were kept in the animal center under regulated conditions (21-24 °C, relative humidity 40%-60%, 12 h light/12 h dark cycle), with free access to food and water. We established an IUA mouse model during the estrous cycle using both mechanical and chemical harm to simulate endometrial injury in the clinical situation. Briefly, the surgery involves mechanical intrauterine operation with a syringe contacting the uterine cavity, as well as chemical injury by intrauterine perfusion with ethanol (95%).[27-29] The mice were randomly assigned into 5 groups (as shown in Supplementary Fig. S1): sham-operated (PBS) group I, in which the uterine cavity was injected with 25 μL PBS and held for 3 min; ethanol group II, for which 25 μL 95% ethanol was injected into the uterine cavity to induce damage for 3 min followed by 25 μL PBS treatment; HP-treated group III, administration of 25 μL HP after endometrium damage by 25 μL 95% ethanol as described above; EXOs treated group IV, administration of 25 μL EXOs (50

μg per uterus) after inducing endometrium damage by 25 μL 95% ethanol; and EXOs-HP–treated group V, administration of 25 μL EXOs-HP (50 μg per uterus) after inducing endometrium damage by 25 μL 95% ethanol. After acclimation for 7 days, the mice were sacrificed for further analyses, as shown in Supplementary Fig. S1. The construction and treatment procedure of the endometrium-injured mouse model are presented in 8 steps, which were briefly described as follows: (1) mouse anesthesia, (2) shaving the back of the mouse, (3) disinfecting exposed areas, (4) uteri exposure, (5) instilling 25 μL ethanol in the uterine cavity and holding 3 min to establish the model of IUA fully, (6) intrauterine instillation of treating materials, (7) muscle suture, and (8) closure of back skin incision.

In Vivo Tracing of CM-DiD-Labeled EXOs

According to the manufacturer's instructions, the commercial red fluorescent probe CM-DiD (US Everbright, Inc., Jiangsu, China) was diluted with DMSO to a storage concentration of 2 mg mL^{-1}. EXOs at a 1000 μg mL^{-1} concentration were suspended in 5 mL PBS containing 2 μg mL^{-1} CM-DiD (Final working concentration). After incubating at 37 °C for 20 min, the labeled exosomes were spun at 120 000*g* for 70 min and then washed with 5 mL PBS at 120 000*g* for 70 min. The CM-DiD-labeled EXOs were then mixed with as-prepared HP. The mouse model was then injected with CM-DiD-labeled EXOs and EXOs-HP, with further detection after transplantation for 0, 1, 3, 7, and 37 days, respectively. Exosome retention duration was evaluated in vivo using an IVIS Spectrum, whilst EXO distribution was measured using IF labeling (observed by an Olympus IX81-FV1000 fluorescence microscope).

Histological Analysis and Immunohistochemistry

Standard H&E staining was used for murine endometrium assessment. Treated female mice were euthanized on day 7 after surgery. The isolated uteri were embedded in paraffin after fixing with 4% paraformaldehyde overnight. The wax blocks were cut into 3-4 μm thick and stained with H&E staining by standard methods to observe the endometrial thickness and the number of glands. Light microscopy photographs (OLYMPUS VS200, Japan) and endometrial images were analyzed using the Application Program Image Pro-Plus (version 6.0). Endometrial area and perimeter were recorded to assess an average measurement of the endometrial thickness (mean endometrial thickness = area/perimeter). Tissue sections were also labeled with Masson's trichrome to measure the degree of endometrial fibrosis by conventional methods. The area of fibrosis was quantified by measuring the area ratio between endometrial stromal fibrosis and the endometrial area using a quantitative image analysis system (Image-Pro Plus software; Media Cybernetics, Bethesda, MD, USA). The IF staining was conducted as previously described.[25] Sections were incubated with primary antibodies Vimentin (5741, Cell Signaling Technology, Boston, USA). The secondary antibody (GK600711; DakoCytomation, Glostrup, Denmark) was applied for 30 min at room temperature. The number of positive staining cells in the glands and stroma was semi-quantitatively scored by the immune response score (IRS) of 2 observers who did not know the source of the samples. The scoring criteria were the same as previously described.[25]

TEM Analysis

For TEM investigations, specimens were fixed in 2.5% glutaraldehyde solution (Sigma-Aldrich Chemie GmbH, Germany) buffered with sodium cacodylate buffer (Sigma-Aldrich Chemie GmbH, Germany) at pH = 7.4 for 2 h at 4 °C. The samples were postfixed for 1 h in 1% osmium tetroxide solution (Agar Scientific, Stansted, UK) at the same temperature and pH, dehydrated at increasing concentrations of ethanol (50%, 70%, 90%, 96%, and 99.5%), in an acetone series and embedded in Epon-812 (Fluka Chemie AG, Buchs, Switzerland) according to standard methods. Semithin sections were stained with methylene blue-azur II to select the region of interest for the following procedures. The semithin sections were analyzed using a Zeiss Axiophot 2 microscope (Zeiss, Germany). The ultrathin (80 nm) sections were cut on the Reichert Om U3 ultratome with a diamond knife (Diatome, Ltd., Biel/Bienne, Switzerland). Sections were mounted on copper grids of mesh size 200 (Sigma-Aldrich Chemie GmbH, Germany) with Perfect Loop (Diatome, Ltd., Biel/Bienne, Switzerland) and stained with uranyl acetate (Agar Scientific, Stansted, UK) and lead citrate (Agar Scientific, Stansted, UK) according to standard methods. For TEM, Tecnai G2 spirit 120 kV frozen TEM was used for viewing and photographing.

SEM Analysis

For SEM examinations, samples were fixed in 2.5% glutaraldehyde solution buffered with sodium cacodylate buffer at pH = 7.4 for 2 h. The specimens were dehydrated in increasing concentrations of ethanol (50%, 70%, 96%, and 99.5%) in an acetone series and dried using a critical point drier. After drying, the samples were mounted on an aluminum stub using silver paint. The samples were then introduced into the chamber of the sputter coater and coated with gold. For SEM, field emission scanning electron microscope Nova nano 450 was used for viewing and photographing.

Fertility Assessment

Treated female mice were mated with fertile males of the same age (female:male = 1:1) 7 days after surgery. The female mice were checked for vaginal plugs the next morning to determine whether pregnancy had occurred. On the 7th day after the initial detection of vaginal plugs, the mice were sacrificed and the location and number of embryo implantation were recorded by photography.

Statistical Analysis

The collected data were analyzed using GraphPad Prism, ver. 8.4.0 software. All results were presented as mean ± SEM. The software compared the means of samples using Student *t* test between 2 groups and one-way analysis of variance (ANOVA) test among multiple groups. *P*-value of $< .05$ was considered statistically significant.

Results

Fibrotic Progression Markers Were Increased in the Endometrium of IUA Patients

A total of 38 patients with moderate-to-severe IUA and 37 patients with normal endometrium were enrolled in our study as the IUA group (IUA) and the control group (CONTROL), respectively. Baseline characteristics were analyzed between

the 2 groups. As shown in Supplementary Table S2, there were no significant differences between the 2 groups regarding age, BMI, and menstrual cycle length. Furthermore, we particularly paid attention to the miscarriage times and endometrial thickness. The results indicated that the miscarriage times were remarkably increased and the endometrial thickness was significantly decreased in the IUA group compared to the CONTROL group.

Pathological examinations of the endometrium in the 2 groups were then performed. First, we characterized the extent of endometrial fibrosis in CONTROL and IUA groups using Masson staining (Fig. 1A). The result showed that the ratio of the area with endometrial fibrosis to the total endometrial area in the IUA group was significantly higher than that in the CONTROL group (16.590 ± 1.240 vs. 50.300 ± 3.563; Fig. 1E). Then we investigated the expression of markers of fibrosis progression including Vimentin, COL5A2 (Collagen Type V Alpha 2 Chain), and COL1A1 (Collagen Type I Alpha 1 Chain) in the endometrium of the IUA group and CONTROL group (Fig. 1B–1D). As shown in Fig. 1F–1H, the expression of Vimentin, COL5A2, and COL1A1 was significantly increased in the endometrium of IUA group compared with the CONTROL group (2.986 ± 0.290 vs. 8.737 ± 0.437, 4.149 ± 0.411 vs. 6.934 ± 0.4174, 3.601 ± 0.323 vs. 6.868 ± 0.532, respectively). In addition, Western blot analysis also showed that endometrium in IUA patients showed significantly higher expression of Vimentin, COL5A2, and COL1A1 compared with normal endometrium (Fig. 1I).

Preparation and Characterization of EXOs-HP

Then, we determined whether HP-MSC-derived EXOs treatment could reverse fibrosis in IUA. Identified HP-MSCs were kindly provided by the College of Life Sciences-iCell Biotechnology Regenerative Biomedicine Laboratory, Zhejiang University (Supplementary Fig. S3). First, we extracted EXOs from HP-MSC. EXOs showed a typical "saucer-like" structure under TEM (Fig. 2A). Western blot showed EXOs-HP expressed surface-specific exosomal markers CD63 and CD81 (Fig. 2B). In addition, EXOs sizes

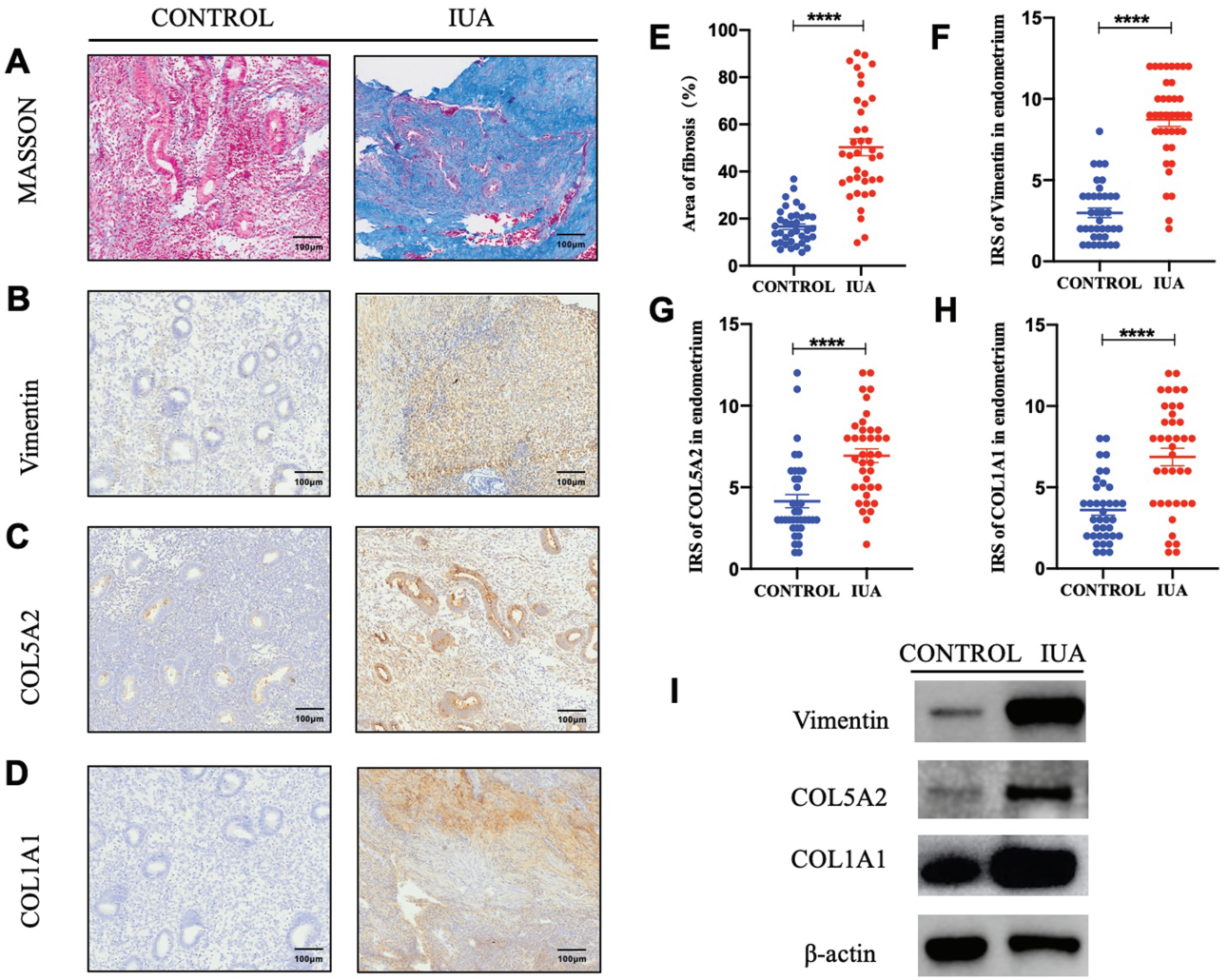

Figure 1. Fibrotic progression markers were increased in the endometrium of IUA patients. (**A**) Masson staining results of human endometrium in the CONTROL and IUA group. (**B-D**) Immunohistochemical staining of Vimentin, COL5A2, and COL1A1 in human endometrium for evaluating fibrosis levels. (**E**) Average fibrosis area and statistical analysis (±SEM) of the 5 groups. The ratio of the fibrotic area = endometrial fibrotic area/endometrial area. ****$P < .0001$, $n = 37$ in CONTROL group, $n = 38$ in IUA group. (**F-H**) Statistic analysis of IRS of Vimentin, COL5A2, and COL1A1 in the endometrium of CONTROL and IUA group. ****$P < .0001$, $n = 37$ in CONTROL group, $n = 38$ in IUA group. (**I**) Representative Western blot analysis of Vimentin, COL5A2, and COL1A1 in the human endometrium of CONTROL and IUA group ($n = 9$).

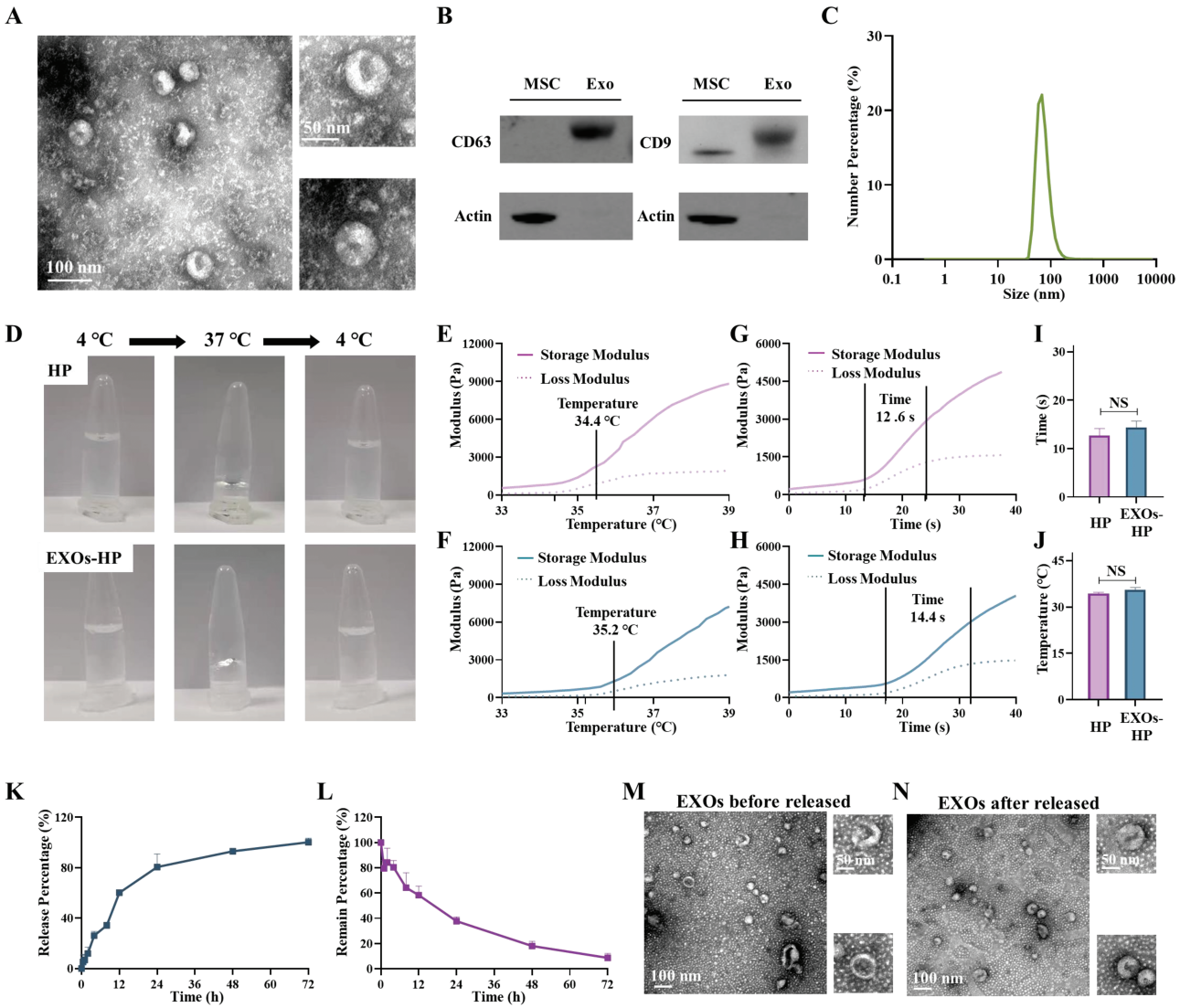

Figure 2. Preparation and characterization of EXOs-HP. (**A**) TEM images of EXOs (3 independent experiments). (**B**) Western blots analysis showing expression of exosome surface markers CD63 and CD9 in HP-MSCs and EXOs. (**C**) DLC size distribution analysis of EXOs (3 independent experiments). (**D**) Visualization of the state of HP and EXOs-HP, respectively, at different temperatures (4 °C, 37 °C, and 4 °C after 37 °C). (**E, F**) *G′* and *G″* changes of HP and EXOs-HP when temperature increased from 30 °C to 42 °C (3 independent experiments). (**G, H**) *G′* and *G″* changes of HP and EXOs-HP when the temperature is at constant 37 °C (3 independent experiments). (**I**) Gelation temperature of HP and EXOs-HP. n.s. indicates $P = .2009$ ($n = 3$, 3 independent experiments). (**J**) Gelation time of HP and EXOs-HP. n.s. indicates $P = .0651$ ($n = 3$, 3 independent experiments). (**K**) Released profile of EXOs-HP at 37 °C in PBS buffer (pH = 7.4; 3 independent experiments). (**L**) Degradation of HP at 37 °C in PBS buffer (pH = 7.4; 3 independent experiments). (**M, N**) TEM images of EXOs before or after being released from HP (3 independent experiments).

range from 50 to 150 nm in diameter, with an average size of 72.34 nm measured by dynamic light scattering analysis (Fig. 2C). These results proved that EXOs were successfully extracted from HP-MSCs.

Poloxamer is commonly used in clinical trials for drug delivery.[30,31] We chose HP as the carrier for EXOs to achieve in situ gelation. To realize gelation of HP in uterine cavity restoration surgery at body temperature, poloxamer 407 concentration of 17.5% (w/w) and poloxamer 188 concentration of 2% were used for HP preparation. HP was fluid at 4 °C, it could quickly form into gel state after incubation at 37 °C and return to fluid when temperature gets back to 4 °C (Fig. 2D). The addition of EXOs did not affect the HP gel phase transition (Fig. 2D). To further explore the phase transition process of HP and EXOs-HP, we employed a rheometer to measure the storage modulus (*G′*) and loss modulus(*G″*) changes of HP and EXOs-HP when temperature increased from 30 °C to 42 °C. The *G′* and *G″* of HP started growing rapidly at 34.4 °C, indicating gel phase transition occurred (Fig. 2E, 2I). Under 37 °C, the gelation of HP only takes 12.6 s (Fig. 2F, 2J), which means HP could fast gelation. After mixing with EXOs, the gelation temperature of HP increased slightly to 35.2 °C, and gelation duration was prolonged to 14.4 s (Fig. 2G, 2H). Nevertheless, there is no significant difference (Fig. 2I, 2J), EXOs-HP still had a preferable gelation temperature and time.

To determine the in vitro release profile of EXOs-HP, fluorescence quantification was used to measure the released exosomes by DiD (Supplementary Fig. S2A). The in vitro profile showed less than 20% EXOs were released within the first 4 h, and ~90% EXOs were released from HP within 48 h (Fig. 2K). Notably, the release profile of EXOs-HP

corresponded to the dissolution curve of HP (Figs. 2L; Supplementary Fig. S2B). Therefore, the incorporation of exosomes with HP could achieve sustained release of EXOs. To further verify the effect of HP on the morphology of EXOs after being released, TEM was conducted. The results showed that the size and morphology of EXOs were unchanged after being released from HP (Fig. 2M, 2N). Western blot analysis also showed that the EXO-associated protein markers of EXOs loaded in HP were not altered after being released from HP (Supplementary Fig. S2C). In conclusion, the incorporation of EXOs with HP did not increase or sustained the release of EXOs.

HP Promoted the Retention of EXOs in the Endometrium of IUA Mice

The optimization of therapeutic efficacy requires the maximized retention of EXOs inside the endometrium. We studied the kinetics of the EXOs being released from HP in IUA mice uterine cavities by non-invasive in vivo imaging (IVIS; ex/em: 644/663). Equal quantities of EXOs and EXOs-HP (50 μg per uterus) labeled by CM-DiD were implanted to the left and right uterus, respectively. As shown in Fig. 3A, more EXOs had retained in the mouse's uterine cavity on the right side than left at 1, 3, 7, and 37 days. Notably, on day 7, the left uterus had few CM-DiD-labeled exosomes, while the right uterus injected with EXOs-HP still had prominent EXOs retention. The result suggested that HP promoted EXOs retention in mice uterus. For further confirmation, we employed ex vivo imaging. Consistent with the in vivo imaging results, more EXOs-HP were retained in the damaged endometrium compared with EXOs (Fig. 3B). In addition, IF indicated that EXOs can infiltrate into the stromal layer in EXOs-HP treated group (Fig. 3C). Taken together, these data indicated that HP can prolong the retention time and promote stromal infiltration of EXOs in IUA endometrium.

EXOs-HP Treatment Restored Functional Endometrium in the IUA Mice Model

To evaluate the therapeutic effect of EXOs-HP in endometrial fibrosis, we established the endometrium-injured mouse model by ethanol perfusion to mimic endometrial injury in real clinical infertile patients.[32,33] Mice were randomized into 5 groups to receive PBS, ethanol, crosslinked HP, EXOs, and

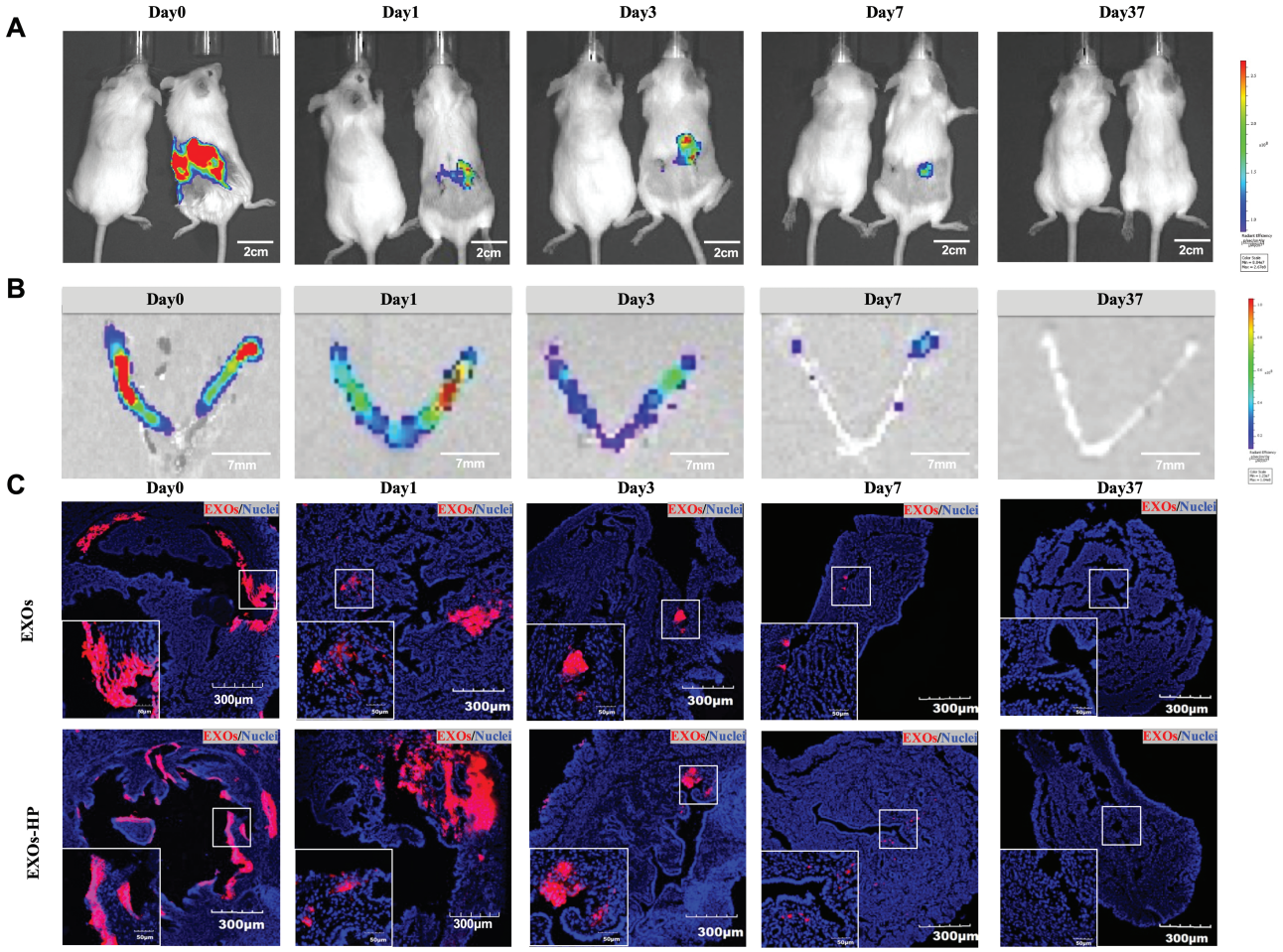

Figure 3. HP promoted the retention of EXOs in the endometrium of IUA mice. (**A**) In vivo fluorescent imaging of mouse at days 0, 1, 3, 7, and 37 after injection. The mouse on the left was the untreated control group to eliminate the interference of autofluorescence, while the mouse on the right was the treatment group. In the treatment group, equal quantities of EXOs and EXOs-HP labeled by CM-DiD were implanted to the left and right uterus, respectively, $n = 3$. (**B**) Ex vivo fluorescent imaging of mouse uteri at days 0, 1, 3, 7, and 37 after injection, $n = 3$. (**C**) Ex vivo continuous frozen section of the uterus showed the retention of exosomes, which were labeled with CM-DiD (red). The nuclei of cells were labeled with DAPI (blue).

EXOs-HP, respectively. A schematic image detailing the animal experiment is presented in Supplementary Fig. S1.

To reveal the morphological changes in the uteri resulting from the treatment, we systematically performed histological analysis of the endometrium 1 week after treatment, including endometrial thickness, degree of fibrosis, and expression of fibrotic progression markers. The endometrium thickness was significantly decreased in the ethanol group compared with the PBS group (123.800 ± 7.820 vs. 240.200 ± 15.200; Fig. 4A). Importantly, EXOs-HP (211.500 ± 26.550) could significantly rescue ethanol induced endometrial damage (Fig. 4F). In addition, the percent of fibrosis area was significantly decreased following EXOs-HP treatment (8.644 ± 0.792) as compared with the ethanol group (13.84 ± 2.093; Fig. 4B, 4G). Furthermore, immunohistochemical staining analysis showed high Vimentin and TGF-β1 expression in endometrial stromal cells in the ethanol group, while EXOs-HP treatments could inhibit both Vimentin and TGF-β1 expression (Fig. 4C, 4D). Finally, we determined the implantation rate by mating treatment IUA mice with normal male mice. The data showed that the number of implanted embryos in the ethanol group is reduced significantly compared to the PBS group (Fig. 4E, 4J). The HP group did not show a significant difference in the number of fetuses compared with the ethanol group. In contrast, the EXOs and EXOs-HP treatment could significantly improve embryo implantation in IUA mice

EXOs-HP Treatment Rescued Endometrial Epithelial and Stromal Cell Morphology in the IUA Mice Model

To determine if EXOs-HP treatment could improve the function of the injured endometrial epithelial and stromal cells, first, we evaluated their effects on the morphology of endometrial cells.

SEM analysis showed that the microvilli of luminal epithelial cells were abruptly destroyed after ethanol treatment. HP and EXOs treatment could rescue the morphology of microvilli to a certain extent (Fig. 5A). EXOs and EXOs-HP treatment could increase microvilli density, while EXOs-HP had the best effective treatment (Fig. 5A). Then we employed TEM to check the structure of glandular epithelial cells and stromal cells. The glandular epithelial cells were covered by many regular short rod-shaped microvilli in the PBS group (Fig. 5B). Similar to luminal epithelial cells, microvilli in glandular epithelial cells were destroyed and irregularly distributed in the ethanol group, while in the EXOs-HP treatment group, the microvilli became uniformly distributed (Fig. 5B). In stromal cells, ethanol treatment led to nucleolytic and pyknosis (Fig. 5C). After treatment with EXOs-HP, the intact nuclear membrane of stromal cells could be restored (Fig. 5C). These results suggested that EXOs-HP treatment could rescue injured endometrial cell morphology.

EXOs Inhibited TGF-β1 Treatment in the IUA Cell Model

To further consolidate the therapeutic effects of EXOs-HP, we used TGF-β1 to induce primary HESCs fibrosis to develop an IUA cell model. We found that TGF-β1 induced primary HESCs fibrosis in a concentration-dependent manner (Fig. 6A). Treatment with 40 ng mL^{-1} TGF-β1 was found to be most effective for developing an IUA cell model, indicated by significantly increased Vimentin, COL1A1, and COL5A2. This was further confirmed by qPCR analysis of fibrotic progression markers, including Vimentin, COL5A2, COL1A1, α-SMA, MMP2, and TGF-βR (Fig. 6B). When treated with 40 ng mL^{-1} TGF-β1, all these markers were significantly increased compared with the control group. Next, we performed IF to further validate the elevation of Vimentin, COL1A1, and COL5A2. Notably, after treating the HESCs with TGF-β1, all these markers were significantly increased (Fig. 6C). Taken together, these data demonstrated that TGF-β1 could induce primary HESCs fibrosis.

To determine the effects of EXOs on TGF-β1 induced primary HESC fibrosis, we added 150 μg mL^{-1} EXOs when treating primary HESC with TGF-β1. Western blot and IF analysis showed that EXOs could significantly downregulate TGF-β1 induced COL1A1 and COL5A2 expression (Fig. 6D, 6F). qPCR also confirmed that Vimentin, COL5A2, COL1A1, α-SMA, MMP2, and TGF-βR were reduced in the TGF-β1 + EXOs group compared with the TGF-β1 group (Fig. 6E). These results indicated that the EXOs treatment could rescue TGF-β1 induced HESC fibrosis.

EXOs Promoted the Proliferation of Human Endometrial Glandular Cell

Endometrial glandular cells are another essential component in the endometrium apart from stromal cells. In IUA patients, the number of glandular cells is decreased, which will result in decreased endometrial thickness and is unfavorable for endometrial receptivity. Then we further explored the effects of exosomes on glandular cell proliferation. Glandular cells were exposed to EXOs for 24 h and then examined by EdU assay. Supplementary Fig. S5A shows glandular cell proliferation rates at 24 h were increased after EXOs treatment when compared to the non-treated group (5.884% ± 0.5852% vs. 2.494% ± 0.6295%; Supplementary Fig. S5B).

Discussion and Conclusion

In this study, we identified 3 upregulated fibrotic progression markers (Vimentin, COL5A2, and COL1A1) in the endometrium of IUA patients and highlighted the efficacious therapy of EXOs-HP via rescuing the fibrosis of endometrium.

It is reported that endometrial fibrosis is the main pathological feature of IUAs, adhesion areas in the uterine cavity show little or no endometrium since it is replaced by dense fibrous tissue.[34,35] Inhibition of endometrial fibrosis is key for the treatment of IUA, since fibrotic change is considered irreversible. The change of Vimentin and Collagen was reported to have a critical role in fibrosis progression.[36-39] Consequently, we explored and found that fibrosis markers including Vimentin, COL1A1, and COL5A2 were upregulated in the endometrium of IUA patients compared to the control group. Similar to our clinical findings, Liu et al. recently discovered that Vimentin and other collagen genes were elevated in IUA patients by microarray sequencing.[40] Together, these findings suggest that the fibrosis process plays an important role in the development of IUA via upregulating Vimentin, COL1A1, and COL5A2, which provided a potential target for therapeutic implications.

IUA therapy aims to reconstruct the normal uterine cavity and restore uterine function.[34] Historically, IUA patients are treated with hysteroscopic resection of adhesions in combination with other adjuvant therapies. However, the shortcomings

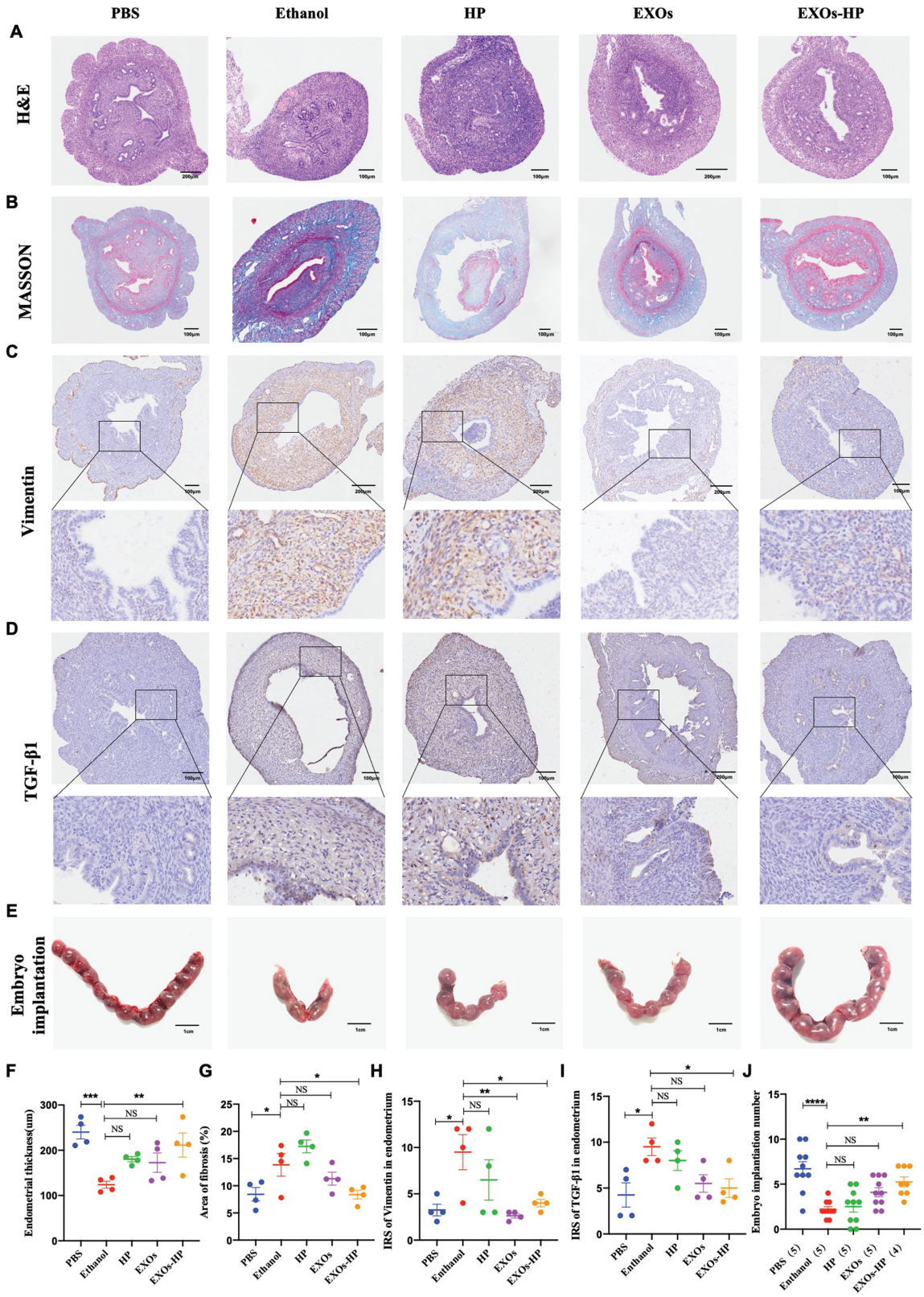

Figure 4. EXOs-HP treatment restored functional endometrium in mice model of intrauterine adhesion. (**A**) H&E staining results of the 5 groups for evaluating the endometrial thickness. (**B**) Masson staining results of the 5 groups for evaluating the endometrial fibrosis area (blue). (**C-D**) Immunohistochemical Vimentin and TGF-β1 expression of the 5 groups. (**E**) The number of implanted embryos in the 5 mouse groups with different treatments. (**F**) Statistical analysis of average endometrial thickness in the 5 groups. *P*-value = .0009 for PBS, *P*-value = .1087 for HP, *P*-value = .1872 for EXOs, *P*-value = .0093 for EXOs-HP, $n = 4$. (**G**) Statistical analysis of the ratio of fibrosis area in the 5 groups. The ratio of the fibrosis area = endometrial fibrotic area/endometrial area. *P* value = .0432 for PBS, *P*-value = .2719 for HP, *P*-value = .1872 for EXOs, *P*-value = .0406 for EXOs-HP, $n = 4$. (**H**) Statistic analysis of IRS of Vimentin in the endometrium of the 5 groups. *P*-value = .0192 for PBS, *P*-value = .4369 for HP, *P* value = .0098 for EXOs, *P* value = .0427 for EXOs-HP, $n = 4$. (**I**) Statistic analysis of IRS of TGF-β1 in the endometrium of the 5 groups. *P*-value = .0120 for PBS, *P*-value = .7246 for HP, *P*-value = .0598 for EXOs, *P*-value = .0318 for EXOs-HP, $n = 4$. (**J**) Statistical analysis of embryo implantation rate. ****P-value < .0001 for PBS, *P*-value = .9874 for HP, *P*-value = .0714 for EXOs, *P*-value = .0030 for EXOs-HP.

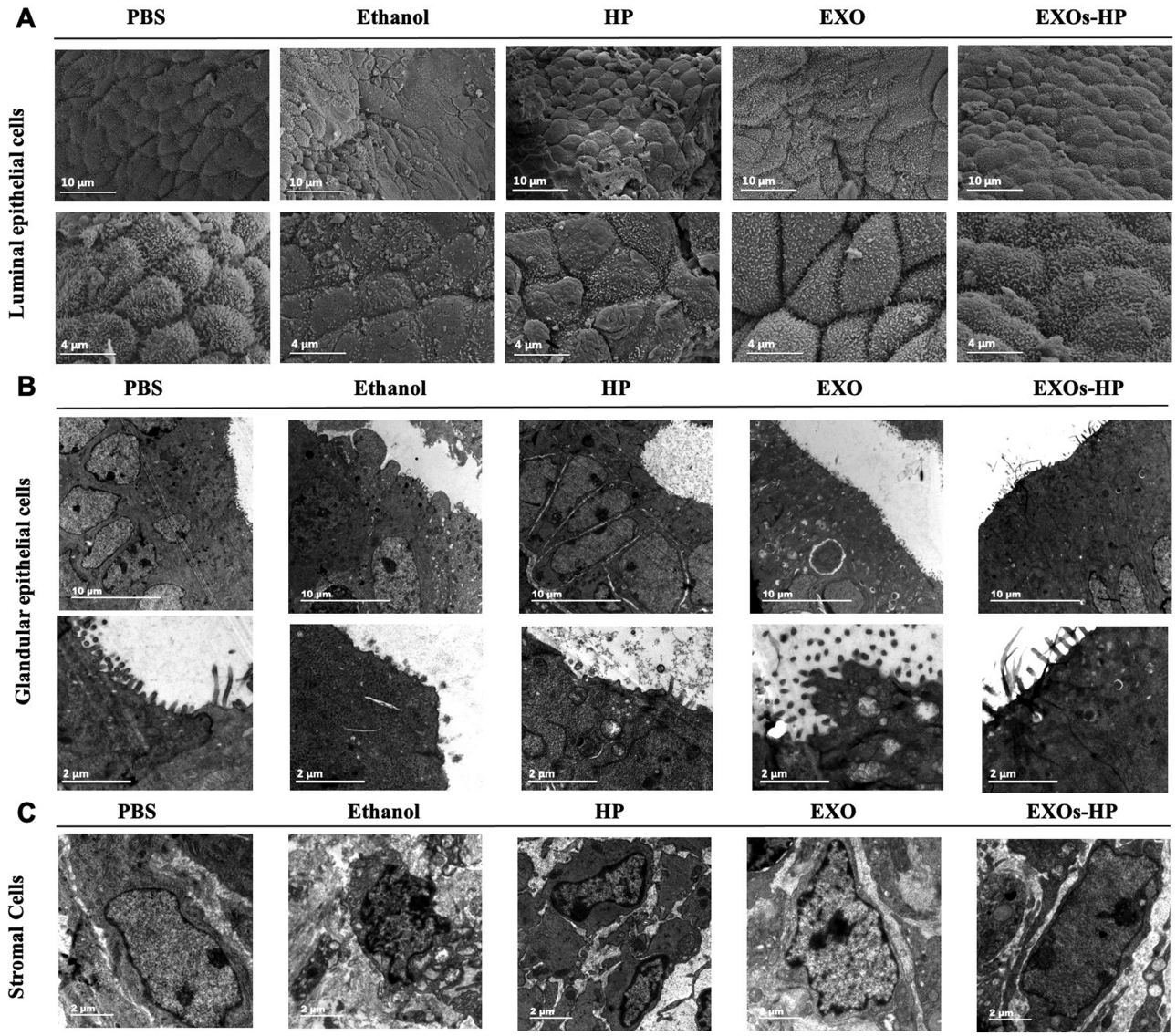

Figure 5. EXOs-HP treatment rescued endometrial epithelial and stromal cell morphology in mice IUA model. (**A**) SEM microphotographs of luminal epithelial cells in 5 groups. The lower row was the magnification of the upper row, 3 independent experiments. (**B**) TEM microphotographs of glandular epithelial cells in 5 groups. The lower row was the magnification of the upper row, 3 independent experiments. (**C**) TEM microphotographs of stromal cells in 5 groups, 3 independent experiments.

of these anti-adhesion strategies include resistance to secondary surgery and endometrial regeneration. Exosome-based therapy has been recently revealed as one of the effective self-repair pathways for many degenerative diseases and has been adopted in clinical trials.[41] For the therapy of intrauterine adhesions by exosomes, there are only a handful of reported cases hitherto, among which bone marrow and adipose mesenchymal stem cell-derived exosomes are principally studied.[13,42] However, bone marrow and adipose tissue are difficult to obtain for large-scale uses owning to the invasive process of collection, which is associated with an increased risk of microbial infection. In contrast, the allogeneic placenta is a bona fide candidate origin of MSCs. The abundant source and non-invasive collection of placenta MSCs make HP-MSC a good candidate for clinical treatment.[43,44] Besides, a recent study indicates that HP-MSCs also show vigorous expansion ability and greater proliferation capacity than umbilical cord-derived MSCs (UC-MSCs).[45] Taken together, all these favorable conditions make HP-MSCs a novel alternative source for stem cell–derived exosome-based therapy in treating intrauterine adhesions.

In clinical operation, endometrial injury in some infertile patients is caused by the intrauterine operation. Correspondently, our animal model is mechanical plus chemical injury model. There is mechanical operation with a syringe in contact with the uterine cavity and chemical degeneration of ethanol in the animal model. Besides, our animal models can cause decreased endometrial thickness, increased fibrosis area, and reduced embryo implantation, which is consistent with real clinical IUA patients to a certain extent. Moreover, this model has also been widely used in previous studies on the endometrium.[46-48]

In most cases, exosomes are delivered by intravenous injection,[49] while we adopted the in situ delivery method to mimic clinical uterine cavity administration for the uterus is closely interlinked with the vagina. However, this delivery

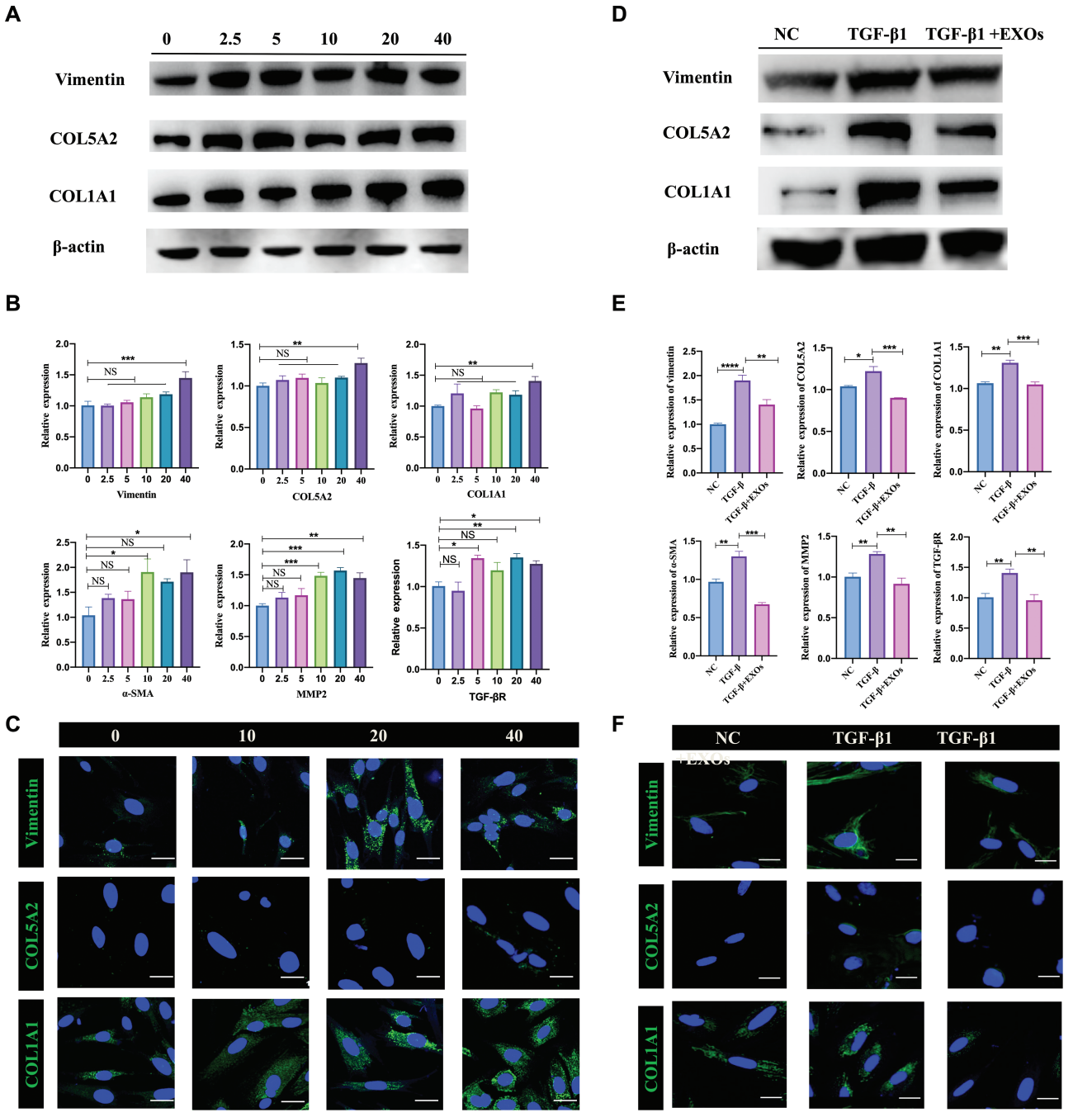

Figure 6. EXOs inhibited TGF-β1 treatment in the IUA cell model. (**A**) Vimentin, COL5A2, COL1A1, and corresponding total protein Western blot analysis in primary HESCs treated with TGF-β1 for various concentrations (0, 2.5, 5, 10, 20, and 40 ng mL^{-1}) at 24 h, 3 independent experiments. (**B**) q-PCR analysis of Vimentin, COL5A2, COL1A1, α-SMA, MMP2, and TGF-βR in primary HESCs treated with TGF-β1 for various concentrations (0, 2.5, 5, 10, 20, and 40 ng mL^{-1}) at 12 h, 3 independent experiments. NS indicates $P > .05$, * indicates $P < .05$, ** indicates $P < .01$, and *** indicates $P < .001$. (**C**) IF analysis of Vimentin, COL5A2, and COL1A1 in HESCs treated with TGF-β1 at different concentrations (0, 10, 20, and 40 ng mL^{-1}), 3 independent experiments. Scale bar = 25 μm. (**D**) Vimentin, COL5A2, COL1A1, and corresponding total protein Western blot analysis in primary HESCs treated with 40 ng mL^{-1} TGF-β1 and 150 μg mL^{-1} EXOs, 3 independent experiments. (**E**) q-PCR analysis of Vimentin, COL5A2, COL1A1, α-SMA, MMP2, and TGF-βR in primary HESCs treated with 40 ng mL^{-1} TGF-β1 and 150 μg mL^{-1} EXOs, 3 independent experiments. NS indicates $P > .05$, * indicates $P < .05$, ** indicates $P < .01$, and *** indicates $P < .001$. (**F**) IF analysis of Vimentin, COL5A2, and COL1A1 in HESCs treated with 40 ng mL^{-1} TGF-β1 and 150 μg mL^{-1} EXOs, 3 independent experiments. Scale bar = 25 μm.

method tends to cause part of the delivered cells/drugs to slip out of the uterus via the vagina, limiting the maximal retention efficacy of cells/drugs. FDA guide has presented HP as an "inactive" ingredient for different types of preparations (eg, IV, inhalation, oral solution, suspension, ophthalmic, or topical formulations).[50-52] Studies have reported that polymer hydrogel is considered a promising strategy to improve wound healing efficiency by increasing the retention time of delivered bioactive ingredient, thus reducing the need for repeated dosing in clinical.[53-55] In our work, exosomes were labeled with 2 μg mL^{-1} CM-DiD, a promising live imaging dye, to trace the retention time. And the result showed that

HP loading could significantly prolong EXOs retention and stability in damaged endometrial tissue. In vivo study also revealed that EXOs-HP could restore the function and structure of injured endometrium, and inhibit fibrosis progress of IUA by downregulating fibrotic progression markers. Therefore, our work demonstrated that EXOs-HP has therapeutic potential for endometrial repair in IUA treatment.

TGF-β1, as a master mediator of fibrosis, is implicated in the pathogenesis of numerous fibrotic diseases by driving the fibrosis process.[56,57] In the present study, we also found increased TGF-β1 expression in the endometrium of IUA model. Therefore, we employed TGF-β1 to induce the IUA cell model to study the molecular mechanisms.[40,58] After applying TGF-β1 to HESCs, the expression of vimentin, COL5A2, and COL1A1 was upregulated, consistent with our previous clinic findings. Besides, we found that EXOs could downregulate the expression of Vimentin, COL5A2, and COL1A induced by TGF-β1. These findings implied that EXOs sufficiently reversed the fibrotic effect of TGF-β1, which provided a solid theoretical foundation for further clinical translation.

In this study, we identified that Vimentin, COL5A2, and COL1A1 were upregulated in the endometrium of IUA patients, which provided a potential target for therapeutic implications. Then, we investigated EXOs-HP in an IUA mice model and discovered that it was capable of significantly restoring the function and structure of the injured endometrium. Similar to the results in vivo, the in vitro IUA cell model suggested that EXOs-HP could restore increased Vimentin, COL5A2, and COL1A1 levels in stromal cells and enhance glandular cell proliferation. However, the precise components of natural exosomes still need to be pinpointed to achieve precision medicine.[59] Besides, further studies could include more advanced animal models like rhesus macaques to better clarify the effects and deeper mechanisms of EXOs-HP treatment. In conclusion, our study provided the theoretical and experimental foundation for the clinical treatment of IUA using EXOs-HP.

Acknowledgments

We thank the College of Life Sciences-iCell Biotechnology Regenerative Biomedicine Laboratory, Zhejiang University for kindly providing us with identified HP-MSCs. We thank C. Yang and D. Song in the Center of Cryo-Electron Microscopy (CCEM), Zhejiang University for their technical assistance on Transmission/Scanning Electron Microscope. We are grateful for the technical support by Q. Huang, J. Chen, and W. Yin of the Core Facilities, Zhejiang University School of Medicine.

Funding

This work was supported by the National Key Research and Development Program of China (2022YFC2703500 and 2018YFC1005003), the National Natural Science Foundation of China (No. 81974224 and No. 81973252), the Key Research and Development Program of Zhejiang Province(2021C03098), Zhejiang Province Science and Technology Plan Projects (LGF22H010006), and Zhejiang Provincial Key Medical Technology Program (WKJ-ZJ-1826).

Conflict of Interest

The authors declared no potential conflicts of interest. All authors have read the journal's policy on disclosure of potential conflicts of interest and declared no conflict of interest. All authors have read the journal's authorship agreement and the manuscript has been reviewed by and approved by all named authors.

Authors Contribution

D.Z., J.-Q.G., Y.-F.L., Y.-S.L., P.-P.C.: conceived and designed the experiments; Y.-F.L., P.-P.C., J.-W.S., X.-Q.L., Y.-Q.W., W.Z., J.L., X.Y.: collected the human endometrial samples; Y.F.L., Y.-S.L., P.-P.C., J.-W.S., Y.-Y.Z., J.-Q.L., J.-N.J., J.-L.X., J.-Y.Z.: performed the experiments; Y.-F.L., Y.-S.L., P.-P.C., J.-W.S., R.-J.Z.: analyzed and interpreted the results; Y.-F.L., Y.-S.L. X.S., C.C., R.-J.Z., J.-Q.G., D.Z.: drafted and revised the manuscript. All authors discussed the results and commented on the manuscript.

Data Availability

The data that support the findings of this study are available from the corresponding author upon reasonable request.

Supplementary Material

Supplementary material is available at *Stem Cells Translational Medicine* online.

References

1. Santamaria X, Isaacson K, Simón C. Asherman's syndrome: it may not be all our fault. *Hum Reprod*. 2018;33(8):1374-1380. https://doi.org/10.1093/humrep/dey232
2. Lee WL, Liu CH, Cheng M, et al. Focus on the primary prevention of intrauterine adhesions: current concept and vision. *Int J Mol Sci*. 2021;22(10):1-20.
3. Ombelet W, Cooke I, Dyer S, Serour G, Devroey P. Infertility and the provision of infertility medical services in developing countries. *Hum Reprod Update*. 2008;14(6):605-621. https://doi.org/10.1093/humupd/dmn042
4. March CM. Management of Asherman's syndrome. *Reprod Biomed Online*. 2011;23(1):63-76. https://doi.org/10.1016/j.rbmo.2010.11.018
5. Westendorp IC, Ankum WM, Mol BW, Vonk J. Prevalence of Asherman's syndrome after secondary removal of placental remnants or a repeat curettage for incomplete abortion. *Hum Reprod*. 1998;13(12):3347-3350. https://doi.org/10.1093/humrep/13.12.3347
6. Ai Y, Chen M, Liu J, et al. lncRNA TUG1 promotes endometrial fibrosis and inflammation by sponging miR-590-5p to regulate Fasl in intrauterine adhesions. *Int Immunopharmacol*. 2020;86:106703. https://doi.org/10.1016/j.intimp.2020.106703
7. Lin X, Chai G, Wu Y, et al. RNA m6A methylation regulates the epithelial mesenchymal transition of cancer cells and translation of snail. *Nat Commun*. 2019;10(1):2065. https://doi.org/10.1038/s41467-019-09865-9
8. Wang P, Luo M-L, Song E, et al. Long noncoding RNA *lnc-TSI* inhibits renal fibrogenesis by negatively regulating the TGF-β/Smad3 pathway. *Sci Transl Med*. 2018;10(462):eaat2039.
9. Di Guardo F, Palumbo M. Asherman syndrome and insufficient endometrial thickness: a hypothesis of integrated approach to restore the endometrium. *Med Hypotheses*. 2020;134:109521. https://doi.org/10.1016/j.mehy.2019.109521
10. Yu D, Wong YM, Cheong Y, Xia E, Li T-C. Asherman syndrome--one century later. *Fertil Steril*. 2008;89(4):759-779. https://doi.org/10.1016/j.fertnstert.2008.02.096

11. Ni J, Liu Y, Kang L, et al. Human trophoblast-derived exosomes attenuate doxorubicin-induced cardiac injury by regulating miR-200b and downstream Zeb1. *J Nanobiotechnol*. 2020;18(1):171. https://doi.org/10.1186/s12951-020-00733-z
12. Yao Y, Chen R, Wang G, Zhang Y, Liu F. Exosomes derived from mesenchymal stem cells reverse EMT via TGF-β1/Smad pathway and promote repair of damaged endometrium. *Stem Cell Res Ther*. 2019;10(1):225. https://doi.org/10.1186/s13287-019-1332-8
13. Zhao S, Qi W, Zheng J, et al. Exosomes derived from adipose mesenchymal stem cells restore functional endometrium in a rat model of intrauterine adhesions. *Reprod Sci*. 2020;27(6):1266-1275. https://doi.org/10.1007/s43032-019-00112-6
14. Lin Y, Dong S, Ye X, et al. Synergistic regenerative therapy of thin endometrium by human placenta-derived mesenchymal stem cells encapsulated within hyaluronic acid hydrogels. *Stem Cell Res Ther*. 2022;13(1):66. https://doi.org/10.1186/s13287-022-02717-2
15. Hu J, Zeng B, Jiang X, et al. The expression of marker for endometrial stem cell and fibrosis was increased in intrauterine adhesious. *Int J Clin Exp Pathol*. 2015;8(2):1525-1534.
16. Xue X, Chen Q, Zhao G, et al. The overexpression of TGF-β and CCN2 in intrauterine adhesions involves the NF-κB signaling pathway. *PLoS One*. 2015;10(12):e0146159. https://doi.org/10.1371/journal.pone.0146159
17. Zhou Q, Wu X, Hu J, Yuan R. Abnormal expression of fibrosis markers, estrogen receptor α and stromal derived factor-1/chemokine (C-X-C motif) receptor-4 axis in intrauterine adhesions. *Int J Mol Med*. 2018;42(1):81-90. https://doi.org/10.3892/ijmm.2018.3586
18. Yue Y, Meng K, Pu Y, Zhang X. Transforming growth factor beta (TGF-β) mediates cardiac fibrosis and induces diabetic cardiomyopathy. *Diabetes Res Clin Pract*. 2017;133:124-130. https://doi.org/10.1016/j.diabres.2017.08.018
19. Huang C, Jing X, Wu Q, Ding K. Novel pectin-like polysaccharide from Panax notoginseng attenuates renal tubular cells fibrogenesis induced by TGF-β. *Carbohydr Polym*. 2022;276:118772. https://doi.org/10.1016/j.carbpol.2021.118772
20. Zhang K, Chen X, Li H, et al. A nitric oxide-releasing hydrogel for enhancing the therapeutic effects of mesenchymal stem cell therapy for hindlimb ischemia. *Acta Biomater*. 2020;113:289-304. https://doi.org/10.1016/j.actbio.2020.07.011
21. Yen B, Hwa H, Hsu P, et al. HLA-G expression in human mesenchymal stem cells (MSCs) is related to unique methylation pattern in the proximal promoter as well as gene body DNA. *Int J Mol Sci*. 2020;21(14):5075.
22. Wu X, Showiheen SAA, Sun AR, et al. Exosomes extraction and identification. *Methods Mol Biol*. 2019;2054:81-91. https://doi.org/10.1007/978-1-4939-9769-5_4
23. Yang D, Zhang W, Zhang H, et al. Progress, opportunity, and perspective on exosome isolation - efforts for efficient exosome-based theranostics. *Theranostics*. 2020;10(8):3684-3707. https://doi.org/10.7150/thno.41580
24. Zhang Y, Bi J, Huang J, et al. Exosome: a review of its classification, isolation techniques, storage, diagnostic and targeted therapy applications. *Int J Nanomed*. 2020;15:6917-6934. https://doi.org/10.2147/IJN.S264498
25. Liu J, Ying Y, Wang S, et al. The effects and mechanisms of GM-CSF on endometrial regeneration. *Cytokine*. 2020;125:154850. https://doi.org/10.1016/j.cyto.2019.154850
26. Li J, Cen B, Chen S, He Y. MicroRNA-29b inhibits TGF-β1-induced fibrosis via regulation of the TGF-β1/Smad pathway in primary human endometrial stromal cells. *Mol Med Rep*. 2016;13(5):4229-4237. https://doi.org/10.3892/mmr.2016.5062
27. Li J, Huang B, Dong L, et al. WJ-MSCs intervention may relieve intrauterine adhesions in female rats via TGF-β1-mediated Rho/ROCK signaling inhibition. *Mol Med Rep*. 2021;23(1):8.
28. Xia L, Meng Q, Xi J, et al. The synergistic effect of electroacupuncture and bone mesenchymal stem cell transplantation on repairing thin endometrial injury in rats. *Stem Cell Res Ther*. 2019;10(1):244. https://doi.org/10.1186/s13287-019-1326-6
29. Xie Y, Tian Z, Qi Q, et al. The therapeutic effects and underlying mechanisms of the intrauterine perfusion of granulocyte colony-stimulating factor on a thin-endometrium rat model. *Life Sci*. 2020;260:118439. https://doi.org/10.1016/j.lfs.2020.118439
30. Casella JF, Barton BA, Kanter J, et al. Effect of poloxamer 188 vs placebo on painful vaso-occlusive episodes in children and adults with sickle cell disease: a randomized clinical trial. *JAMA*. 2021;325(15):1513-1523. https://doi.org/10.1001/jama.2021.3414
31. Abdeltawab H, Svirskis D, Sharma M. Formulation strategies to modulate drug release from poloxamer based in situ gelling systems. *Expert Opin Drug Deliv*. 2020;17(4):495-509. https://doi.org/10.1080/17425247.2020.1731469
32. Zhang S, Sun Y, Jiang D, et al. Construction and optimization of an endometrial injury model in mice by transcervical ethanol perfusion. *Reprod Sci*. 2021;28(3):693-702.
33. Huang J, Zhang W, Yu J, et al. Human amniotic mesenchymal stem cells combined with PPCNg facilitate injured endometrial regeneration. *Stem Cell Res Ther*. 2022;13(1):17. https://doi.org/10.1186/s13287-021-02682-2
34. Zhu HY, Ge TX, Pan YB, Zhang S-Y. Advanced role of hippo signaling in endometrial fibrosis: implications for intrauterine adhesion. *Chin Med J (Engl)*. 2017;130(22):2732-2737. https://doi.org/10.4103/0366-6999.218013
35. Santamaria X, Cabanillas S, Cervelló I, et al. Autologous cell therapy with CD133+ bone marrow-derived stem cells for refractory Asherman's syndrome and endometrial atrophy: a pilot cohort study. *Hum Reprod*. 2016;31(5):1087-1096. https://doi.org/10.1093/humrep/dew042
36. Hatipoglu OF, Uctepe E, Opoku G, et al. Osteopontin silencing attenuates bleomycin-induced murine pulmonary fibrosis by regulating epithelial-mesenchymal transition. *Biomed Pharmacother*. 2021;139:111633. https://doi.org/10.1016/j.biopha.2021.111633
37. Livingston MJ, Shu S, Fan Y, et al. Tubular cells produce FGF2 via autophagy after acute kidney injury leading to fibroblast activation and renal fibrosis. *Autophagy*. 2022;1(19):22.
38. Verrecchia F, Rossert J, Mauviel A. Blocking sp1 transcription factor broadly inhibits extracellular matrix gene expression in vitro and in vivo: implications for the treatment of tissue fibrosis. *J Invest Dermatol*. 2001;116(5):755-763. https://doi.org/10.1046/j.1523-1747.2001.01326.x
39. Corbel M, Belleguic C, Boichot E, Lagente V. Involvement of gelatinases (MMP-2 and MMP-9) in the development of airway inflammation and pulmonary fibrosis. *Cell Biol Toxicol*. 2002;18(1):51-61. https://doi.org/10.1023/a:1014471213371
40. Liu L, Chen G, Chen T, et al. si-SNHG5-FOXF2 inhibits TGF-β1-induced fibrosis in human primary endometrial stromal cells by the Wnt/β-catenin signalling pathway. *Stem Cell Res Ther*. 2020;11(1):479. https://doi.org/10.1186/s13287-020-01990-3
41. Kwon H, Yang S, Lee J, et al. Combination treatment with human adipose tissue stem cell-derived exosomes and fractional CO_2 laser for acne scars: a 12-week prospective, double-blind, randomized, split-face study. *Acta Derm Venereol*. 2020;100(18):adv00310.
42. Yao Y, Chen R, Wang G, Zhang Y, Liu F. Exosomes derived from mesenchymal stem cells reverse EMT via TGF-β1/Smad pathway and promote repair of damaged endometrium. *Stem Cell Res Ther*. 2019;10(1):225. https://doi.org/10.1186/s13287-019-1332-8
43. Park S, Koh SE, Hur CY, et al. Comparison of human first and third trimester placental mesenchymal stem cell. *Cell Biol Int*. 2013;37(3):242-249. https://doi.org/10.1002/cbin.10032
44. Zhu SF, Zhong ZN, Fu XF, et al. Comparison of cell proliferation, apoptosis, cellular morphology and ultrastructure between human umbilical cord and placenta-derived mesenchymal stem cells. *Neurosci Lett*. 2013;541:77-82. https://doi.org/10.1016/j.neulet.2013.03.018
45. Feng X, Liu J, Xu Y, et al. Molecular mechanism underlying the difference in proliferation between placenta-derived and umbilical cord-derived mesenchymal stem cells. *J Cell Physiol*. 2020;235(10):6779-6793. https://doi.org/10.1002/jcp.29572

46. Huang J, Zhang W, Yu J, et al. Human amniotic mesenchymal stem cells combined with PPCNg facilitate injured endometrial regeneration. *Stem Cell Res Ther.* 2022;13(1):17. https://doi.org/10.1186/s13287-021-02682-2
47. López-Martínez S, Rodríguez-Eguren A, de Miguel-Gómez L, et al. Bioengineered endometrial hydrogels with growth factors promote tissue regeneration and restore fertility in murine models. *Acta Biomater.* 2021;135:113-125. https://doi.org/10.1016/j.actbio.2021.08.025
48. Zhang L, Li Y, Guan CY, et al. Therapeutic effect of human umbilical cord-derived mesenchymal stem cells on injured rat endometrium during its chronic phase. *Stem Cell Res Ther.* 2018;9(1):36. https://doi.org/10.1186/s13287-018-0777-5
49. Habib S, Singh M. Recent advances in lipid-based nanosystems for gemcitabine and gemcitabine-combination therapy. *Nanomaterials*. 2021;11(3):597.
50. Dumortier G, Grossiord JL, Agnely F, Chaumeil JC. A review of poloxamer 407 pharmaceutical and pharmacological characteristics. *Pharm Res*. 2006;23(12):2709-2728. https://doi.org/10.1007/s11095-006-9104-4
51. Date AA, Halpert G, Babu T, et al. Mucus-penetrating budesonide nanosuspension enema for local treatment of inflammatory bowel disease. *Biomaterials*. 2018;185:97-105. https://doi.org/10.1016/j.biomaterials.2018.09.005
52. Rowe R, Sheskey P, Owen S. Pharmaceutical Handbook of Pharmaceutical Excipients, 5th edn., Pharmaceutical, London, UK and American Pharmaceutical Association, Washington, USA. 2005.
53. Wu J, Zhu J, He C, et al. Comparative study of heparin-poloxamer hydrogel modified bFGF and aFGF for in vivo wound healing efficiency. *ACS Appl Mater Interfaces*. 2016;8(29):18710-18721. https://doi.org/10.1021/acsami.6b06047
54. Hui Q, Zhang L, Yang X, et al. Higher biostability of rh-aFGF-carbomer 940 hydrogel and its effect on wound healing in a diabetic rat model. *ACS Biomater Sci Eng*. 2018;4(5):1661-1668. https://doi.org/10.1021/acsbiomaterials.8b00011
55. Malik MI, Lee S, Chang T. Comprehensive two-dimensional liquid chromatographic analysis of poloxamers. *J Chromatogr A*. 2016;1442:33-41. https://doi.org/10.1016/j.chroma.2016.03.008
56. Leask A, Abraham DJ. TGF-beta signaling and the fibrotic response [in eng]. *FASEB J*. 2004;18(7):816-827. https://doi.org/10.1096/fj.03-1273rev
57. Nasu K, Nishida M, Matsumoto H, et al. Regulation of proliferation, motility, and contractivity of cultured human endometrial stromal cells by transforming growth factor-beta isoforms. *Fertil Steril*. 2005;1114:1123.
58. Zhu H, Pan Y, Jiang Y, et al. Activation of the Hippo/TAZ pathway is required for menstrual stem cells to suppress myofibroblast and inhibit transforming growth factor β signaling in human endometrial stromal cells. *Hum Reprod*. 2019;34(4):635-645. https://doi.org/10.1093/humrep/dez001
59. Kalluri R, LeBleu VS. The biology, function, and biomedical applications of exosomes [in eng]. *Science*. 2020;367(6478):eaau6977.